Effect of 3-D Printing on Mechanical Properties of Poly(vinyl alcohol) based Algal Biopolymer Composites

Pranav Krishnan
MANOJIT DAS
manojit.mech@gmail.com

IIT Kharagpur: Indian Institute of Technology Kharagpur https://orcid.org/0000-0003-3888-5433
Rushikesh S. Ambekar
Himanshu Singh
Sehmus Ozden
Chandra Sekhar Tiwary

Research Article

Keywords: Direct Ink Writing, Biocomposites, Solvent Casting, Polymer Films, Microalgae

Posted Date: February 2nd, 2026

DOI: https://doi.org/10.21203/rs.3.rs-8651682/v1

Abstract

A significant challenge of the 21st century is to develop sustainable and environmentally friendly materials that also exhibit high strength. One key strategy is to utilize naturally derived resources to manufacture Biocomposites. These consist of a bio-derived reinforcement for strength within a biodegradable matrix, drastically mitigating the environmental impact in their manufacture and disposal. In this work, a novel poly (vinyl alcohol) (PVA) composite reinforced with Chlorella microalgae (*Chlorella Salina*) is developed to fabricate films using the Direct Ink Writing 3D printing technique. Mechanical properties and structural characteristics of these 3D printed composites are benchmarked against those prepared by traditional solvent casting. The 3D printed samples demonstrate superior mechanical performance, primarily attributed to more uniform particle dispersion and directionally oriented microalgae reinforcements within the polymer matrix. Incorporating microalgae into printable PVA-based inks opens future possibilities for developing sustainable packaging materials and complex 3D structures.

1. Introduction

In today's world, plastics are the primary antagonist in two dire problems: first, most major polymers are derived from petroleum, which causes a large carbon footprint [1], and is getting scarce in itself; second, the enormous problem of plastic waste since most common plastics are not biodegradable.[2, 3] Plastic waste disposal by landfill or incineration causes damage to the environment and human health, while land and water pollution annually by plastics is only increasing. [4] Due to these factors, biopolymers are of huge scientific and industrial interest - polymers that are derived from renewable raw material (biomass, agricultural waste etc.), and are biodegradable. Biopolymer-based composites are a sustainable alternative to traditional composites used in packaging, construction and the automobile industries that offer a reduction in cost, weight, and carbon footprint. Various biomass-based reinforcements have been used to fabricate composites in recent years, like chitin[5], cellulose[6], and wheat gluten.[7] However, only about 1% of annual plastic production in the world consists of bioplastics. [8] This is due both to the lack of economical mass-production and because the primary biomass sources today are from terrestrial crops like potato or corn - this competes with the food supply, making bioplastics a less appetizing prospect.[9, 10] A potential solution to these problems is to utilize microalgae as an alternative biomass source.

Microalgae are microscopic, aquatic plant-like organisms, ranging in size from a few micrometers to a few hundred micrometers. They differ from macroalgae in that they are unicellular as opposed to multicellular and cannot be seen by the naked eye. They can grow on waste resources and have a high capacity for carbon capture.[11, 12] Microalgae have been shown in recent years to have good potential to be blended with polymers to form strengthened bio-polymer composites. [9, 13, 14] Chlorella Salina (Chl.) is one of the most promising candidates - it has a higher thermal stability and crack resistance than

other species due to its dense cell walls.[15, 16] In addition, it has a high utilization of incident light energy, leading to fast growth and a CO_2 fixing rate of over 1 kg/day.[17]

Enhancing the efficacy of microalgae in biopolymer composites can be achieved by embracing nontraditional manufacturing techniques, such as additive manufacturing. This approach offers both material handling flexibility and the potential to enhance mechanical strength. 3D printing offers numerous advantages over traditional manufacturing methods, as highlighted by Ligon et al.[18] These include greater design freedom, faster product development cycles, rapid on-demand manufacturing, and lower startup costs. One of the most significant benefits of 3D printing is its ability to produce complex parts within a single machine without the need for specialized tools, a process that differs from the material removal or casting and assembly typical in traditional manufacturing. Additionally, 3D printing presents a more sustainable approach to manufacturing by minimizing material consumption: only the material used for the actual assembly of the product, passing through the printer's extruder, is consumed. Despite the progress made in 3D printing technology over recent decades, the predominant materials utilized remain metal, ceramic, or petroleum-derived plastics.[19] This limitation hampers the widespread adoption of the technology in certain sectors. For instance, issues such as the production of toxic by-products and the lack of biodegradability or biocompatibility in synthetic materials impede the utilization of 3D printing in biomedical applications. By integrating the principles of 3D printing with those of bio-based renewable materials, there is an opportunity to foster a sustainable and renewable bioeconomy across various sectors.

Extrusion-based 3D printing is being developed for a wide range of material classes, including polymers, metals, and ceramics. The traditional Fused Filament Fabrication (FFF) method has the limitation of only being able to print structures using filaments made from standard materials such as Polylactic acid (PLA) or Acrylonitrile Butadiene Styrene (ABS). The Direct ink writing (DIW) technique offers a much larger range of material choice, allowing the printing of complex structures made from novel composite materials, with tunable properties.[20] Any material can be printed if it has the requisite rheological properties – a fluid with a yield stress sufficient to provide adequate shape retention.[21, 22] Chlorella has been previously shown to impart yield-stress behavior in aqueous suspensions and emulsion-based inks by Kwak et al.[23] In particular, the control over the directionality and distribution of reinforcement particles offered by DIW is of great interest.[24, 25] This microstructural control during synthesis can be utilized to obtain agglomeration-free and preferentially oriented particulate composites with enhanced structural properties.[25]

Yoon et al. have demonstrated water purification by 3D printing microbial biocarriers using Chlorella vulgaris with alginate /methylcellulose hydrogels.[26] Uribe-Wandurraga’s outcomes derived from this study can offer valuable insights into how the inclusion of microalgae in batter affects the process of, and subsequent impact on the post-processing of 3D-printed food products. The optimized ink provided not only better mechanical properties but also good geometrical accuracy.[27] Microalgae represents a sustainable solution for development, offering a renewable reservoir of diverse materials well-suited for

3D printing purposes. Scientists have endeavored to explore the 3D print capabilities of materials derived from algae and their potential for 4D bioprinting applications. Extensive research has been conducted on microalgae possessing 3D printing capabilities along with shape memory effects, shedding light on their implications.[28] Zhao and team printed robust 3D structures using silk and microalgae. This study opens new possibilities for enhancing indoor air quality by increasing oxygen levels and decreasing carbon dioxide to promote a greener, healthier environment indoors.[29]

Polyvinyl alcohol (PVA) is a biodegradable polymer that is a strong candidate for water-soluble films and composites due to its relatively high tensile strength (~ 48 MPa).[30, 31] It is synthesized from acetic acid and ethylene, which can be derived from a renewable biomass source to make the obtained PVA a bio-derived polymer.[13] It is an ideal candidate to develop colloidal suspension inks for Direct Ink Writing due to good mixing and interfacial interaction with reinforcement particles, particularly organic polymer molecules, as demonstrated by Sabathini et al.[32, 33] Hence, developing a polymer composite composed of PVA and reinforced by Chlorella offers the possibility of a completely biobased composite with improved thermal and mechanical properties, which can be printed to form complex 3D structures. From previous studies, it has been established that PVA can be used to prepare biocompatible inks along with other different reinforcement materials (graphite, eggshell, chicken bone extract, SiC, etc.) for biomedical applications having enhanced mechanical strength.[34–36]

In this study, a custom PVA/Chlorella ink was developed for DIW by obtaining a viscous fluid with optimal viscosity and homogeneity for printing sustainable biopolymer films. A comparative study of chlorella particle distribution and its effect on mechanical properties using 3D printing and solvent casting was conducted. Additionally, the impact of 3D printing in both transverse and longitudinal directions was examined, offering the potential to tune the ultimate strength of the printed composite. Fourier-transform Infrared Spectroscopy (FTIR) was conducted, and the obtained spectra analyzed to determine what covalent bonds were present at the interface between the PVA matrix and the Chlorella filler particles. An experimental setup for characterization was developed to compare the two fabrication routes of Direct ink writing and Solvent casting. Tensile film samples with dimensions corresponding to ASTM standards were both 3D printed and solvent cast using the same ink. Mechanical testing of each composition was conducted, and the performance of the printed and cast samples compared. Finally, the fracture surfaces were inspected by Scanning Electron Microscopy to obtain further information about the deformation behavior of the films.

2. Experimental Details

2.1 Materials

Polyvinyl alcohol pellets produced by Sigma-Aldrich were used. The PVA had an average molecular weight of 130,000 g/mol. and was 99+% hydrolyzed. *Chlorella Salina* microalgae was obtained from Seagrass Tech Pvt. Ltd. in the form of a powder with broken cell walls with an average particle size of 5–

10 µm. The algae were collected off the coast of Karaikal, Pondicherry, India and then dried and powdered.

2.2 Methods

2.2.1 Ink Synthesis

A weighed amount of PVA and Chlorella (in the desired wt% ratio) was premixed and ground with a mortar and pestle for 10 minutes to get a homogenous solid mixture. This mixture was stirred into deionized water at 80°C using a mechanical stirrer to obtain a 15 wt% PVA solution in water (w/v).[22] Four inks were prepared of 0.5 wt%, 1 wt% and 5 wt% of Chlorella in PVA, as well as a PVA solution with no chlorella as baseline to observe the effects of the reinforcement. After the ink was prepared it was filtered through a 0.2 mm sieve to remove large undissolved particles. It was then allowed to settle for 12–16 hours to allow the dissipation of air bubbles incorporated during mixing, which would interfere with the printing process.

2.2.2 Direct Ink Writing

The Hyrel Engine HR® 3D Bioprinter was used to print the prepared PVA/Chl. ink. A 200 mm/min printing speed with layer thickness of 1 mm was used. Tensile specimens with specific dimensions as per ASTM: D882-18 standards (gauge length = 70 mm, width = 10 mm, thickness = 0.1 mm) were created using SolidWorks® and then sliced using Slic3r. The printed samples solidified on the print bed at room temperature (25°C) and pressure for 15 minutes.

2.2.3 Solvent Casting

The PVA/Chl. ink was used to make tensile samples of the same standard dimensions, using a film applicator. A drop of ink was spread evenly across the surface of a glass slide, by moving the film applicator manually to obtain a thickness of 0.2 mm. The cast samples were then dried and allowed to solidify in a vacuum desiccator at room temperature (25°C).

2.3 Characterization

2.3.1 Transmission Optical Microscopy

Transmission optical microscopy (Radical Scientific Equipments - RTC-7 Series®) was used to observe the film microstructure since the samples were thin and translucent. In the brightfield imaging mode, micrographs of both the sample microstructures as well as fracture surfaces were captured at 4x, 10x, 20x and 40x magnification.

2.3.2 Fourier-transform Infrared Spectroscopy

FTIR spectroscopy was conducted using a Bruker® Lumos II FTIR Spectrometer. The peaks in the absorption spectra were compared to corresponding peaks in a database of the bonds present in the structure, to determine changes at the particle-matrix interface after 3D printing.

2.3.3 Tensile Testing

A Hounsfield® (H10KS) Universal Testing Machine (UTM) was used for tensile testing of the fabricated samples. Uniaxial loading was performed at 10mm/min, until failure. Since the applied force and measured stresses were expected to be low (< 10 N and < 20 MPa respectively), a sensitive load cell of 500N was used.

2.3.4 Scanning Electron Microscopy

Fracture surface analysis of the samples after tensile testing was conducted using a JEOL® JSM-IT300HR Scanning Electron Microscope (SEM). The samples that showed the best mechanical properties via the solvent cast and direct writing modes of fabrication respectively (0.5 wt% cast and 5 wt% printed longitudinal) were sputtered with gold. The standard high voltage vacuum mode of operation was used with an operating voltage of 3.0 kV, to obtain images using a Secondary Electron Detector (SED). The SEM micrographs were then analyzed to determine their mode of failure, and the role of their respective microstructures in the failure.

3. Results and Discussion

3.1 Structure and Morphology

Transmission optical microscopy was used to determine the particle size, particle distribution and defects present in the PVA/Chl. composite, by observing the microstructures of both the solvent cast and 3D printed samples. In the solvent cast sample (Fig. 1b), it is immediately visible that agglomeration occurs even for solid loading as low as 0.5 wt%. Average particle size (7.49 μm feret diameter) was marginally larger than the printed sample (5.86 μm), and mean Coefficient of Variation (CV) for particle distribution was larger as well (19.35% vs. 16.95%) indicating less uniformity (Table S1).

In the comparison of microstructures of the printed samples in Fig. 1 (c-d), the first visible difference is the homogeneous distribution of Chlorella particles. Agglomeration is low to negligible even as the solid loading increases by ten times to 5 wt%. The second distinct feature is the particle directionality. The particles are observed to be aligned in the direction of printing, either longitudinal or transverse with respect to the rectangular dimensions of the tensile specimen. Direct ink-writing is known to cause preferential particle orientation, and this is observed in the higher particle aspect ratio in 3D printing compared to solvent casting (1.96 vs. 1.63, Table S1). Results of measured sample shrinkage and calculated porosity are discussed in section S.2.5.

3.2 Particle-matrix interface

Fourier-transform infrared spectroscopy (FTIR) was employed to investigate potential interactions between Chlorella microalgae particles and the poly(vinyl alcohol) (PVA) matrix. Spectra were collected for pure Chlorella, pure PVA, and PVA composite films containing different microalgae concentrations (0.5%, 1%, and 5% wt%). The captured absorption spectra are represented in Fig. 1e to compare the

peaks of the formulations and ascertain end-group physical interactions at the interface of chlorella particles and PVA matrix.[37, 38] Significant peaks around 1682 cm^{-1} and 1475 cm^{-1} correspond to amide-related functional groups (C = O stretching and N-H bending, respectively), indicative of proteinaceous components inherent to Chlorella. These characteristic bands allow us to monitor changing interactions at the algae-polymer interface, as the intensity increases with Chl. loading. Additionally, peaks associated with hydroxyl groups (broad peak around 3480 cm^{-1}) were observed, indicating possible hydrogen bonding between hydroxyl groups on PVA and carbonyl-containing functional groups on Chlorella.[30]

A peak near 2356 cm^{-1}, initially observed, may be attributed to environmental CO_2 interference rather than the formation of isocyanate groups. Future controlled analyses are required to clarify its exact origin.

Overall, observed FTIR patterns suggest effective physical interaction, primarily from hydrogen bonding, between the PVA matrix and Chlorella particles. This interaction could potentially be enhancing interface compatibility and mechanical performance in the composites.

3.3 Mechanical performance in tension

The engineering stress-strain curves obtained by the UTM on tensile loading of the samples, and the mechanical properties (Ultimate tensile strength (UTS), Yield strength (YS), Fracture strain (FS) and Fracture toughness (FT)) calculated using them in Fig. 2 give a comprehensive idea about the tensile mechanical performance of the PVA/Chlorella composite films. We expect an enhanced tensile strength in the composites compared to the virgin PVA films due to an interfacial reaction between the reinforcement and polymer matrix facilitating a stress transfer to the reinforcement particles. The strength of the interface interactions between PVA matrix and chlorella particles reinforcement is the key factor that determines how well the two materials are bonded together, and this turns in affect the overall strength of the composite material. One of the most important factors that can influence the strength of the interface interactions is the presence of functional groups on the surface of the chlorella particles. These functional groups can interact with the PVA molecules, forming non-covalent hydrogen bonding via carbonyl groups on the surface of chlorella particles and hydroxyl groups on the surface of PVA matrix.

While the solvent cast samples have a comparable tensile strength to the printed samples without reinforcement, there is a stark difference as Chl. wt% increases, due to the deterioration of mechanical properties on agglomeration (Fig. 2 (a-b)). On the other hand, the 3D printed samples display a uniform rise in strength and toughness (Fig. 2 (c-d)) as the Chl. wt% increases, proving its efficacy as a reinforcement particle. While this rise is not linear, this could be due to the composite approaching its saturation point of reinforcement addition. Further studies and tests are required to obtain a numerical relation between the amount of Chlorella reinforcement and its effect on mechanical performance.

The 3D printed samples also display significantly improved fracture strain (Figure S3-d), easily withstanding strains 30–90% larger than cast samples with the same Chl. wt%. This is due to the bigger plastic zone as compared to elastic zone, observed in the corresponding stress-strain curves.

A very distinct effect of printing directionality is also observed in the mechanical performance of the 3D printed samples with Chlorella reinforcement: The **longitudinal** samples display higher tensile strength and fracture toughness as compared to transverse samples of the same Chl. wt% (Fig. 3 (c-d)). The reason for this could be twofold: 1) The total surface area of the interfaces between lines of printing is **lower** in the longitudinal samples, where only 10–12 parallel lines are required to print the entire sample. As opposed to transverse samples that require close to seven times as many lines (since $l = 7 \times w$); 2). These interfacial regions in the longitudinal samples are **perpendicular** to the direction of loading, while they are parallel to the loading direction for transverse samples. Since the interfacial regions are weaker and depend on adhesion between the layers (which in turn is a function of rheology, physical interactions, and solidification kinetics), this could also be a reason for the difference in mechanical behavior.

3.4 Fracture surfaces and mechanism

The fracture surfaces for the solvent cast samples in Fig. 4 (a-b) reveal that the primary cause for failure is not the fracturing of the reinforcement, but rather due to the defects present after solidification such as holes, bubbles, and tears. The surfaces are also quite flat, indicating a brittle-like fracture. This could be the cause of very low fracture toughness and strain of cast samples, observed in Fig. 2 (g-h). As Chl. wt% is increased, a very stark concentration gradient is observed (Fig. 4b), with Chlorella particles agglomerating at the fracture surface prior to failure.

On the other hand, the fracture surfaces of the 3D printed samples in Fig. 4(c-f) display a distinct ‘cup and cone’ geometry, indicative of ductile fracture. This could be the reason for high fracture toughness and strain values as well as a relatively lower yield stress (Fig. 2f), since the plastic region of deformation is much larger than the elastic.

Chlorella agglomeration at the fracture surface is also observed in this case: with a higher concentration of particles only at the surface for 0.5 wt% chlorella, whereas a discernible concentration gradient across the sample length is observed for the higher solid loading of 5 wt% (Fig. 4(e-f)). The increase in mean CV – from 16.95% to 52.35% for the printed sample and from 19.35% to 40.02% for the cast sample – clearly displays this particle agglomeration on force loading. Since defects in the printed samples are less prevalent, they do not have much of an influence on their failure.

The effect of printing directionality is also interesting to note. Due to the loading being in the longitudinal direction, Chlorella particles even in the transverse samples change their orientation to align with the loading direction. This is observed in Fig. 4e and 4f, where darker regions of agglomeration are observed after loading, in the loading direction rather than the direction of printing: a change caused by the reorientation of reinforcement particles due to the applied force. This reorientation on loading is

corroborated by an increase in particle aspect ratio after fracture, from 1.96 to 2.25 (Table S1). While the transverse samples are weaker than their longitudinal counterparts, the difference is low (< 10%). This could possibly be due to the particle reorientation compensating for the interfacial weakness since Chlorella cells are spherical.

Scanning electron microscopy performed on the fracture surfaces (thickness of samples) sheds further light on the possible mechanism of failure [39]. The smoother surface for the cast sample (Fig. 4g) compared to the rougher surface for the printed sample (Fig. 4i) indicates the differing fracture mechanisms (brittle vs. ductile). The presence of distorted and damaged Chlorella particles on the surface of printed samples (Fig. 4j) also shows the reason for strengthening could be that they take on more of the load, compared to the intact cells in cast samples (Fig. 4h).

4. Conclusion

A comparative study of PVA-Chlorella composites synthesized by solvent casting and Direct Ink Writing was conducted. The results showed that 3D printing creates a more homogeneous distribution of Chlorella particles without particle agglomeration, which allowed for higher weight fractions of reinforcement without a decrease in mechanical properties. 3D printing also produced fewer defects, resulting in improved mechanical performance due to the better interfacial interactions and stress transfer between PVA matrix and chlorella particles. The directionality of the 3D printed samples also influenced their mechanical properties, with samples printed in the longitudinal direction displaying better tensile properties than those printed in the transverse direction. Further work can explore the effect of varying printing parameters such as nozzle size and extrusion pressure, on microstructure of the films and the resulting mechanical properties.

The emergence of Direct Ink Writing as a technique to fabricate novel polymer composites brings great possibilities for the functional applications of these composites. The developed PVA/Chl. composite has potential in two areas in particular: heavy metal remediation from wastewater, and as a piezoelectric material. The biocompatibility and biodegradability of this composite also bring about crucial advantages in its deployment in ecologically sensitive or biomedical use cases.

Declarations

Declaration of Funding

There is no funding for the current project.

Declaration of Competing Interest

The authors declare that they have no known competing financial interests or personal relationships that could have appeared to influence the work reported in this paper.

Authors’ contributions

P.K. drafted, edited, and compiled the manuscript. R.S.A. and H.S. performed 3D printing. S.O. did SEM, and FTIR did the supervision and proofreading. M.D. and C.S.T. analyzed and finalized the draft.

Acknowledgements

Thanks to the Rubber Technology Centre, Indian Institute of Technology, Kharagpur for performing the tensile tests on the 3D printed and solvent cast polymer composite films.

Data availability statement

All the data available in the article have been provided with proper links and citations. Still if required the data underlying this article will be shared on reasonable request to the corresponding authors. Data is provided in the manuscript and supporting information.

References

1. Cabernard L, Pfister S, Oberschelp C, Hellweg S (2022) Nat Sustain 5. 10.1038/s41893-021-00807-2
2. Geyer R, Jambeck JR, Law KL (2017) Sci Adv 3. 10.1126/sciadv.1700782
3. Rastogi RP, Madamwar D, Pandey A (2017) *Algal Green Chemistry: Recent Progress in Biotechnology*
4. Okunola A, Kehinde I AO, Oluwaseun A, Olufiropo A (2019) E J Toxicol Risk Assess 5. 10.23937/2572-4061.1510021
5. Davila-Rodriguez JL, Escobar-Barrios VA, Shirai K, Rangel-Mendez JR (2009) J Fluor Chem 130. 10.1016/j.jfluchem.2009.05.012
6. Sousa S, Costa A, Silva A, Simões R (2019) Polym (Basel) 11. 10.3390/polym11010066
7. Ciapponi R, Turri S, Levi M (2019) Materials 12. 10.3390/ma12091476
8. Cinar SO, Chong ZK, Kucuker MA, Wieczorek N, Cengiz U, Kuchta K (2020) Int J Environ Res Public Health 17. 10.3390/ijerph17113842
9. Rahman A, Miller CD (2017) in *Algal Green Chemistry: Recent Progress in Biotechnology*
10. Zeller MA, Hunt R, Jones A, Sharma S (2013) J Appl Polym Sci 130. 10.1002/app.39559
11. Yousuf A (2019) *Microalgae Cultivation for Biofuels Production*
12. Sayre R (2010) Bioscience 60. 10.1525/bio.2010.60.9.9
13. Zanchetta E, Damergi E, Patel B, Borgmeyer T, Pick H, Pulgarin A, Ludwig C (2021) Algal Res 56:102288
14. Chiellini E, Cinelli P, Ilieva VI, Martera M (2008) Biomacromolecules 9. 10.1021/bm701041e

15. Dianursanti SA, Khalis (2018) in *E3S Web of Conferences*
16. Dianursanti M, Gozan C, Noviasari (2018) in *E3S Web of Conferences*
17. Zia KM, Zuber M, Ali M (2017) *Algae Based Polymers, Blends, and Composites: Chemistry, Biotechnology and Materials Science*
18. Ligon SC, Liska R, Stampfl J, Gurr M, Mülhaupt R (2017) Chem Rev 117. 10.1021/acs.chemrev.7b00074
19. Ngo TD, Kashani A, Imbalzano G, Nguyen KTQ, Hui D (2018) Compos B Eng 143. 10.1016/j.compositesb.2018.02.012
20. Lewis JA (2006) Adv Funct Mater 16. 10.1002/adfm.200600434
21. Lewis JA (2006) 10.1002/adfm.200600434
22. Smay JE, Cesarano J, Lewis JA (2002) Langmuir 18. 10.1021/la0257135
23. Kwak C, Young Ryu S, Park H, Lim S, Yang J, Kim J, Kim JH, Lee J (2021) J Colloid Interface Sci 582. 10.1016/j.jcis.2020.08.007
24. Rocha VG, Saiz E, Tirichenko IS, García-Tuñón E (2020) J Mater Chem Mater 8. 10.1039/d0ta04181e
25. Wright WJ, Koerner H, Rapking D, Abbott A, Celik E (2022) Compos B Eng 236. 10.1016/j.compositesb.2022.109814
26. Yoon SW, Kim SY, Jeon JS, Oh S, Chung SY, Kim JS, Maeng SK (2024) J Water Process Eng 57. 10.1016/j.jwpe.2023.104711
27. Uribe-Wandurraga ZN, Zhang L, Noort MWJ, Schutyser MAI, García-Segovia P, Martínez-Monzó J (2020) Food Bioproc Tech 13. 10.1007/s11947-020-02544-4
28. Grira S, Khalifeh HA, Alkhedher M, Ramadan M (2023) Bioprinting 33. 10.1016/j.bprint.2023.e00291
29. Zhao S, Guo C, Kumarasena A, Omenetto FG, Kaplan DL (2019) ACS Biomater Sci Eng 5. 10.1021/acsbiomaterials.9b00554
30. Tran DT, Lee HR, Jung S, Park MS, Yang JW (2018) Algal Res 31. 10.1016/j.algal.2016.08.016
31. Jain N, Singh VK, Chauhan S (2017) J Mech Behav Mater 26. 10.1515/jmbm-2017-0027
32. Sabathini HA, Windiani L, Dianursanti M, Gozan (2018) in *E3S Web of Conferences*
33. Jiang P, Yan C, Guo Y, Zhang X, Cai M, Jia X, Wang X, Zhou F (2019) Biomater Sci 7. 10.1039/c9bm00081j
34. Das M, Jana A, Dixit A, Mishra R, Maity S, R K, Basha SS, Maiti P, Panda SK, Arora A, Owuor PS, Tiwary CS (2023) Ceram Int 49. 10.1016/j.ceramint.2023.06.220
35. Das M, Jana A, R K, Swarnkar R, Dixit A, Panda SK, Kumar S, Devasia R, Tiwary CS (2024) ACS Appl Eng Mater 2:2549
36. Das M, Jana A, Mishra R, Maity S, Maiti P, Panda SK, Mitra R, Arora A, Owuor PS, Tiwary CS (2023) ACS Appl Bio Mater 6. 10.1021/acsabm.2c01075
37. Lamnawar K, Baudouin A, Maazouz A (2010) Eur Polym J 46. 10.1016/j.eurpolymj.2010.03.019

38. Keplinger T, Cabane E, Chanana M, Hass P, Merk V, Gierlinger N, Burgert I (2015) Acta Biomater 11. 10.1016/j.actbio.2014.09.016

39. Ferrer-Balas D, Maspoch ML, Mai YW (2002) Polym (Guildf) 43. 10.1016/S0032-3861(02)00102-7

Figures

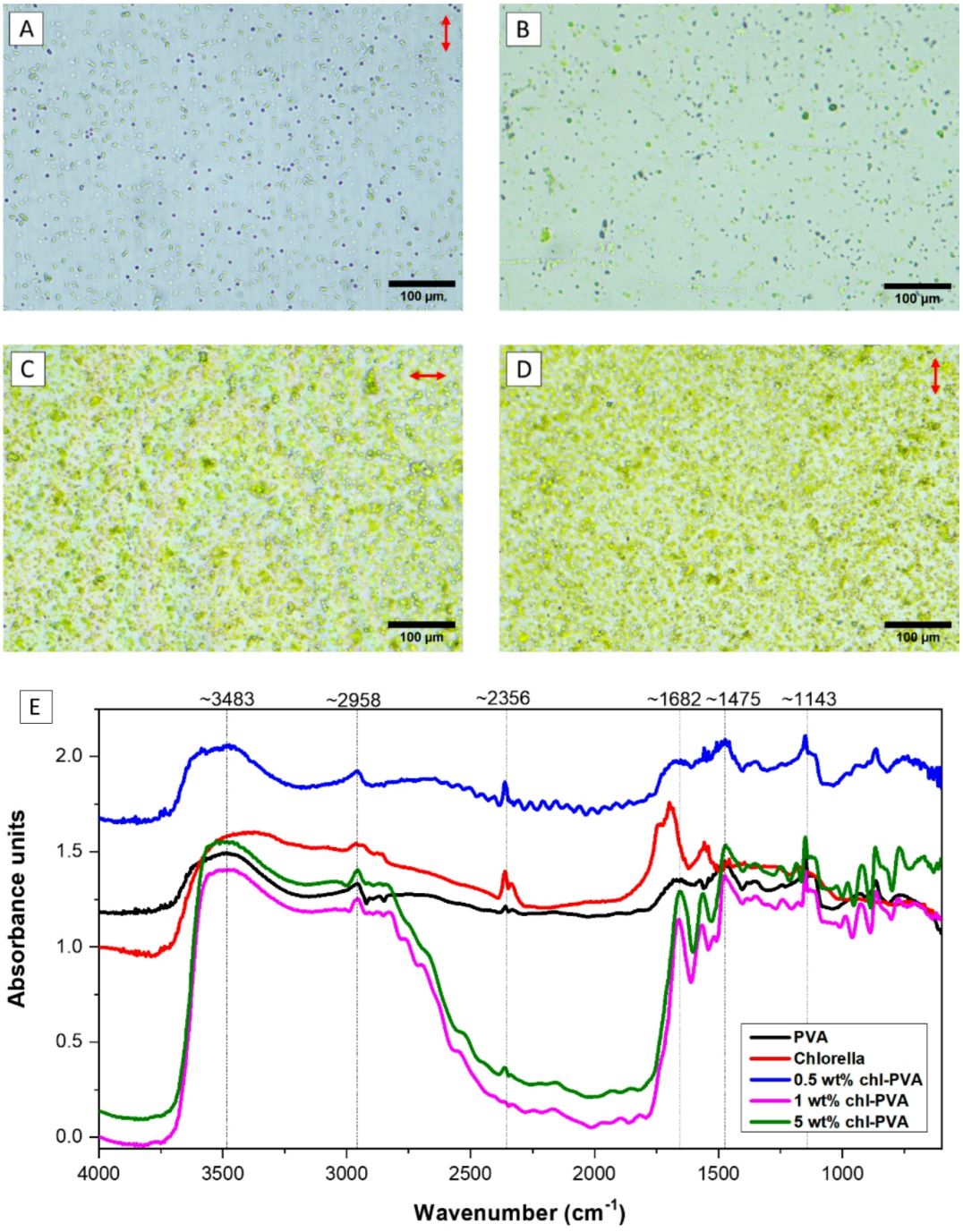

Figure 1

Transmission optical micrographs of PVA-Chlorella composites of composition (a) 0.5 wt% chl. 3D printed, (b) 0.5 wt% chl. solvent cast, (c) 5 wt% chl. printed (longitudinal), (d) 5 wt% chl. printed (transverse). (e) FTIR spectra of the base materials and studied composite formulations. Red arrow indicates direction of 3D printing.

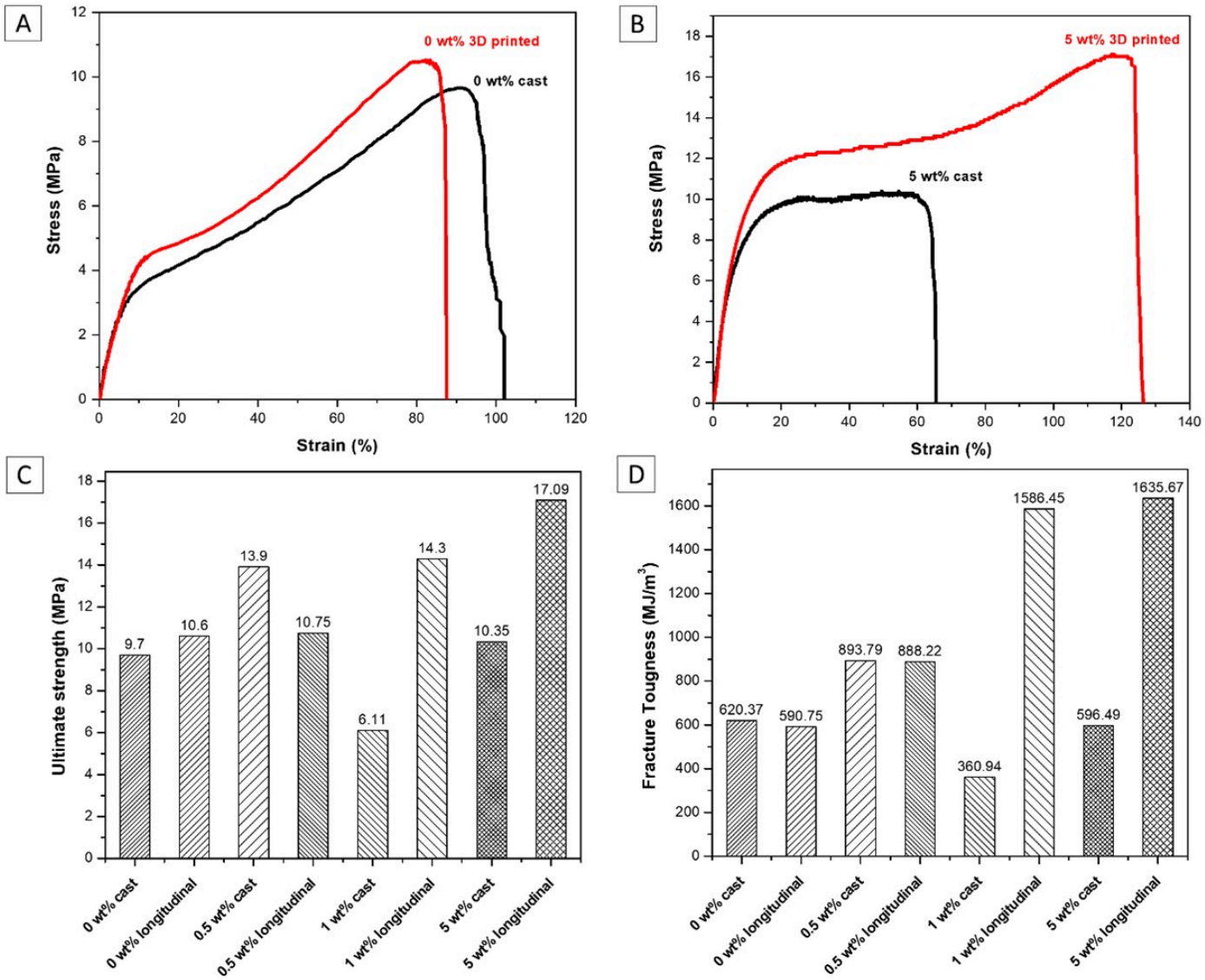

Figure 2

Stress vs. Strain plots obtained by tensile tests on PVA-Chlorella composite films analyzing the **effect of fabrication method**: Solvent Casting vs. Direct-Ink Writing (longitudinal direction). Sample composition (a) 0 wt% chl, (b) 5 wt% chl; Comparison of mechanical properties of solvent cast and 3D printed samples of varying composition: (c) Ultimate tensile strength, (d) Fracture toughness.

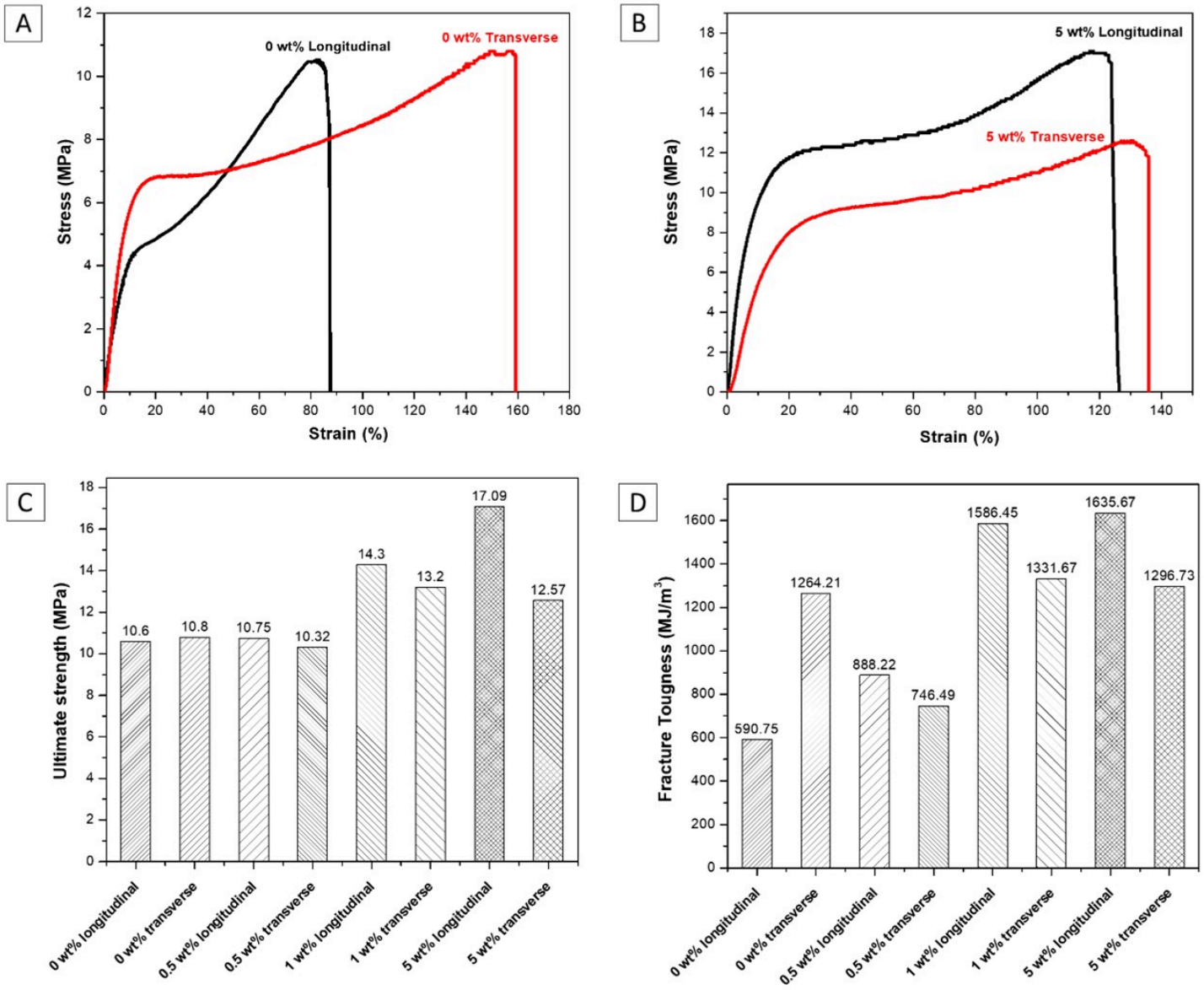

Figure 3

Stress vs. Strain plots obtained by tensile tests on PVA-Chlorella composite films analyzing the **effect of printing direction** in Direct-Ink Writing (Transverse direction vs. Longitudinal direction with respect to sample orientation). Sample composition (a) 0 wt% chl, (b) 5 wt% chl; Comparison of mechanical properties of 3D printed samples of varying composition, printed in transverse and longitudinal orientations: (c) Ultimate tensile strength, (d) Fracture toughness.

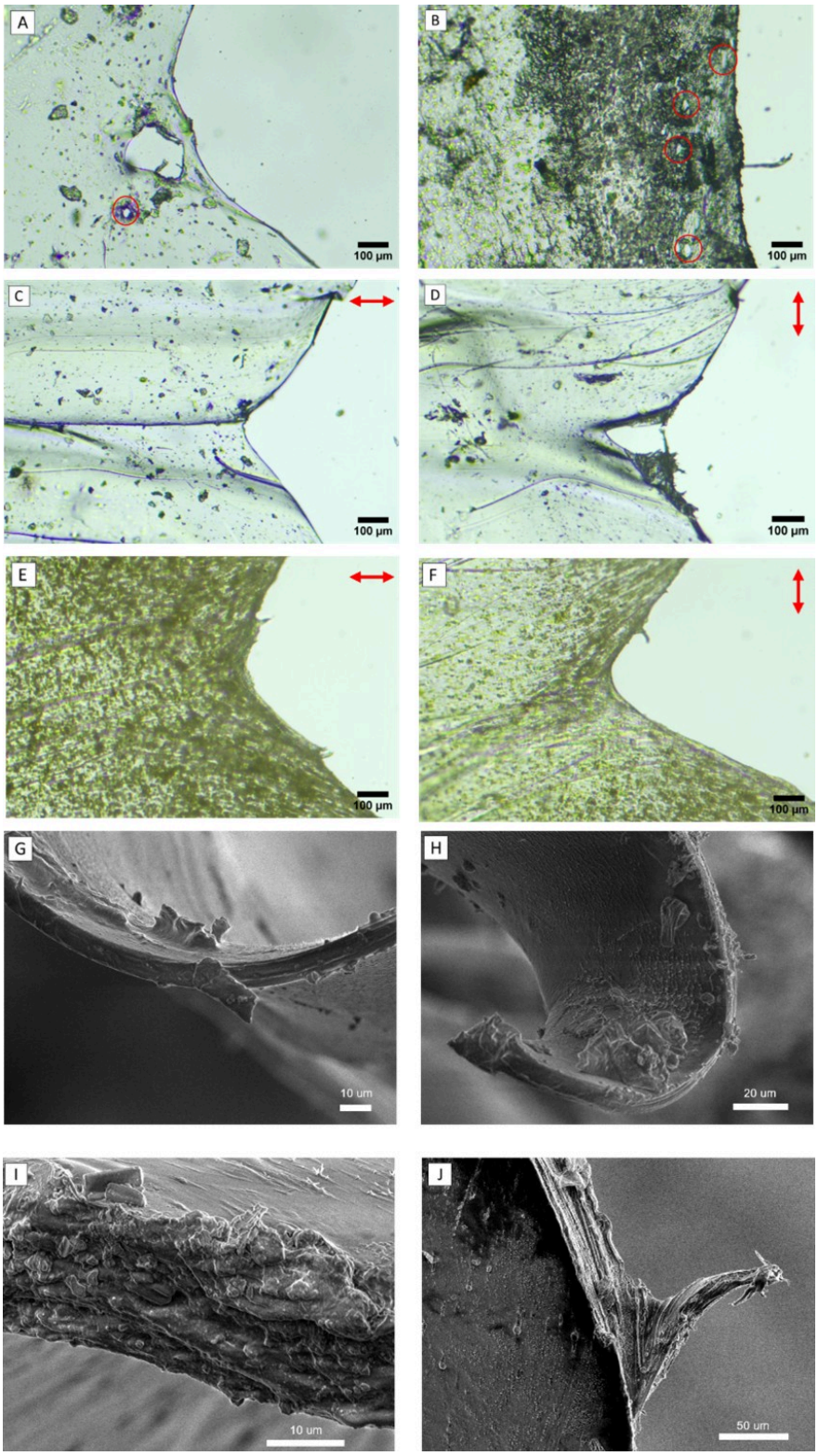

Figure 4

Transmission optical micrographs of the face of fractured samples: Solvent cast films of: (a) 0.5 wt% chl, (b) 5 wt% chl; 3d Printed films of: (c) 0.5 wt% chl. longitudinal, (d) 0.5 wt% chl. transverse, (e) 5 wt% chl. longitudinal, (f) 5 wt% chl. transverse; Scanning electron micrographs of the thickness of fracture surfaces: (g-h) 0.5 wt% chl. solvent cast, (i-j) 5 wt% chl. 3D printed (longitudinal). Red circles indicate voids in cast samples that act as stress concentrators. Red arrow indicates direction of 3D printing.

Supplementary Files

This is a list of supplementary files associated with this preprint. Click to download.

- GAtext.docx
- Supportinginformation.docx
- graphicalabstract.png